Vol 16 No 8, August 2007
1009-1963/2007/16(08)/2433-06
Chinese Physics
© 2007 Chin. Phys. Soc.
and IOP Publishing Ltd

# Theoretical research on enhancement of gain for Ni-like Ag 13.9 nm x-ray laser using a new two-layer target*

Zhang Guo-Ping(张国平), Zhang Tan-Xin(张覃鑫), Zheng Wu-Di(郑无敌), and Qiao Xiu-Mei(乔秀梅)

*Institute of Applied Physics and Computational Mathematics, Beijing* 100088, *China*

(Received 27 September 2006; revised manuscript received 23 November 2006)

For experiments such as on Ni-like Ag x-ray laser, driven by $1\omega$ laser, the gain region is only several nm depth near the target surface, this paper proposes a new two-layer target, in which a thin layer (several nm depth) of silver is plated on the surface of some other materials. Furthermore, the Ni-like Ag 13.9 nm x-ray laser produced by three new kinds of two-layer target with CH, Al and Ge as foundation, was theoretically studied.

**Keywords:** x-ray laser, Ni-like Ag, Ne-like Ge, simulation
**PACC:** 4255V, 5250J, 5265, 8220W

## 1. Introduction

The wavelengths of Ni-like Pd and Ag x-ray Laser (XRL) were 14.7 and 13.9 nm respectively. Using these laser lines as probe light, the electronic density near the critical surface were diagnosed by Mach-Zehnder interferometer in the Lawrence Livermore National Laboratory (LLNL) and the Shanghai Institute of Laser Plasma (SILP) respectively.[1−4] But the brightness of XRL was relatively weaker than that of spontaneous radiation from middle and high $Z$ plasma near the critical surface, so that only the electronic density in the low $Z$ as CH plasma could be diagnosed. In order to increase space resolution and diagnose middle and high $Z$ plasma near the critical surface, it is necessary to increase the brightness and the coherence of XRL. Therefore, it is necessary to increase the gain in Ni-like ions XRL, to get deeply saturated gain, to increase output energy and to improve laser beam quality.

In experiments such as on Ni-like Ag XRL, driven by 1 $\omega$ laser with 100 ps duration, the gain region was located $\sim 100$ $\mu$m from the target surface with electron density of about $10^{19}$ cm$^{-3}$.[5] In this sense, most laser energies were wasted, so that Dunn *et al* proposed a concept of grazing incidence technique in the transient collisional scheme.[6] We think that this kind of technique may be adapted to the quasi-steady state (QSS) collisional scheme with 100ps laser duration.[7,8] Since the gain region is only several nm depth near the target surface initially, we wonder whether if a thin layer of silver ($\sim$ several nm depth) was plated on some other materials we could get higher gain. We call this kind of target a two-layer target. Using our series code,[9] this paper studies Ni-like Ag XRL produced by using this two-layer target. Three different kinds of targets with CH, Al and Ge as foundation are considered.

## 2. Optimization to silver thickness on Ni-like Ag 13.9 nm laser line

The driving laser was a 100 ps Gaussian pulse, with 95 J energy, at 1.053 $\mu$m wavelength, and it was preceded by a 1 % prepulse, and both pulses are in normal incidence. The interval between the peak of prepulse and main pulse $t_{12}$ was 2.5 ns. The line focus was 22 mm long and 100 $\mu$m wide, the target was 20 mm flat target. In order to consider plasma aging in simulating XRL transport and amplification, the XRL photon meets different plasma status after travelling 1 ps. The optimization to silver thickness $d_{\rm Ag}$ was performed. The absorption ratio of driving laser $\eta_{\rm a}$, the maximum electron temperature in the plasma $T_{\rm emax}$ and the effective gain $G_{\rm ef}$ for 13.9 nm line vs. $d_{Ag}$ are shown in Figs.1(a) and 1(b) respectively. For pure silver target, $\eta_{\rm a}$, $T_{\rm emax}$ and $G_{\rm ef}$ were 67.5 %, 1919 eV and 12.8 cm$^{-1}$ respectively. For two-layer target, $\eta_{\rm a}$ and

*Project supported by the National High Technology Research and Development Program of China (Grant No AA847010).

$T_{\rm emax}$ decreased. When $d_{\rm Ag}$ was 2.4 nm, $\eta_{\rm a}$ and $T_{\rm emax}$ were 29.0 % and 1208 eV with CH foundation, 42.1 % and 1552 eV with Al foundation, and 66.0 % and 1823 eV with Ge foundation respectively. For target with Ge foundation these were close to those for pure silver target. When $d_{\rm Ag}$ was 4.8 nm for the three different targets, they increased to 30.6 % and 1262 eV, 44.8 % and 1587 eV, and 66.5 % and 1816 eV, respectively. For each target, when $d_{\rm Ag}$ increased to 11.4 nm, 9.0 nm and 4.8 nm respectively, $\eta_{\rm a}$ was close to that for pure silver target. When $d_{\rm Ag}$ further increased, $\eta_{\rm a}$ could be sometimes a little bigger than that for pure silver target. It was due to a weak shock wave at the interface of two different layers when the main pulse came. It also resulted in the fluctuation of $T_{\rm emax}$ and $G_{\rm ef}$.

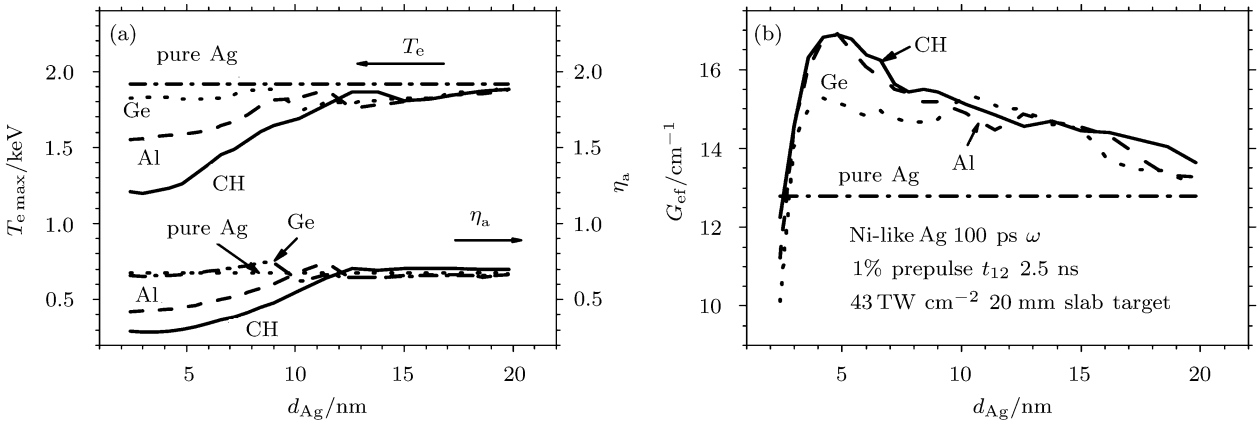



**Fig.1.** (a) $T_{\rm emax}$ and $\eta_{\rm a}$ vs. $\rm d_{Ag}$. (b) Optimization to $d_{\rm Ag}$ for 13.9 nm line.

As $d_{\rm Ag}$ increased, $G_{\rm ef}$ quickly increased to a maximum and then slowly decreased. For the two-layer target with CH and Al foundation, $G_{\rm ef}$ varies very similarly, and they both reached the maximum 16.9 cm$^{-1}$ at $d_{\rm Ag} = 4.8$ nm, about 30 % bigger than that for pure silver target. For two-layer target with Ge foundation, when $d_{\rm Ag}$ was 4.2 nm, its $G_{\rm ef}$ reached maximum 15.3 cm$^{-1}$, which is 20 % larger than that for pure silver target.

## 3. Analysis and discussions about the results of two-layer target

Firstly, we study Ni-like Ag 13.9 nm laser line. For pure silver target, the model was Agn3. At $t_{\rm p} = 6$ ps (the peak time of main pulse is taken as zero ps) XRL photon contributing to output peak intensity arrived at the middle of target, the plasma status of the gain region at this time and time evolution of gain was shown in Figs.2(a) and 2(b) respectively. It showed that near the critical surface, electron temperature $T_{\rm e}$ had a quite flat top with ∼1820 eV. But plasma here was over ionized and the abundance of Ni-like ions $\eta_{\rm Ni}$ was very small. The gain region was $\sim 60 - 70$ $\mu$m (initial target surface is taken as zero $\mu$m). In gain region $T_{\rm e}$ was from 670 eV down to 420 eV, it was only 28 % of that near the critical surface. The maximum gain $G_{\rm p}$ was 16.6 cm$^{-1}$, and its position $x_{\rm p}$ was 66.7 $\mu$m. There $T_{\rm e}$, ion temperature $T_{\rm i}$, $\eta_{\rm Ni}$, and electronic density $N_{\rm e}$ were 504 eV, 27.8 eV, 37.0 % and $4.17\times10^{19}$ cm$^{-3}$ respectively.

For model Agn3 the full width at half maximum (FWHM) of gain region d$x$ was 11.3 $\mu$m. The average gradient of electron density d$N_{\rm e}$/d$x$ was $-1.99 \times 10^{22}$ cm$^{-4}$ in gain region. For the 13.9 nm XRL line, the gradient of refracted angle $d\theta/{\rm d}z$ was 1.72 mrad/cm, here $z$ is the distance in the axial direction. For half target length, the refracted angle $\theta_1$ was 1.72 mrad, and the deflected distance $x_1$ was 8.6 $\mu$m, approaching to ∼76 % of d$x$. From Fig.2(b), the gain region incessantly moved outside. It lasted 100 ps, when $G_{\rm p}$ was bigger than 12 cm$^{-1}$. From 6 to 66ps, the gain region moved 17.2 $\mu$m, the average moving angle $\theta_2$ was 0.96 mrad, the total refracted angle $\theta = \theta_1 + \theta_2$ was 2.68 mrad, and the corresponding $\theta_{\rm ph}$ calculated by series codes was 2.61 mrad. For half target length, the distance $x_2$ that the peak gain moved was 9.6 $\mu$m. The position of peak output XRL intensity in near field $x = x_1 + x_2 + x_{\rm p}$, was 84.9 $\mu$m, and the corresponding $x_{\rm ph}$ calculated by series codes was 85.4 $\mu$m.

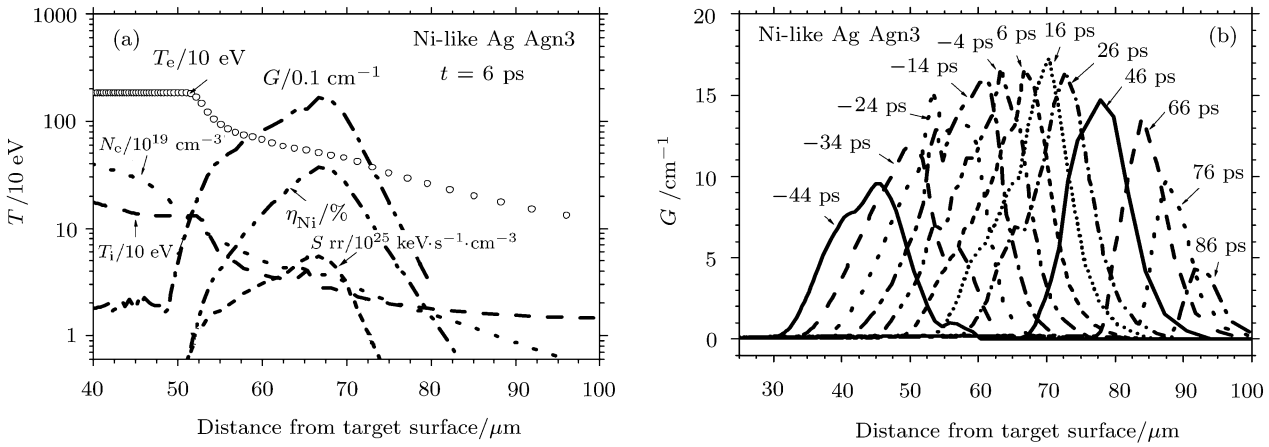



**Fig.2.** (a) Plasma status of gain region. (b) Time evolution of gain for model Agn3.

For the two-layer target with CH foundation, the model B5n3 with $d_{Ag}$ = 4.8 nm was best. $t_p$ was 11 ps, and the plasma status of gain region at this time and the time evolution of gain are shown in Figs.3(a) and 3(b) respectively. This reveals that two smoothly varying regions appeared on the curve for electron temperature; one was near critical surface, with ∼1200 eV, and another was in the silver plasma, with ∼ 880 eV. Here plasma was over ionized and $\eta_{Ni}$ was low. The gain region was ∼ 65−80 $\mu$m. In gain region $T_e$ was from 870 eV down to 500 eV, it was ∼50 % of that near the critical surface. The gain region incessantly moved outside. It lasted 110 ps, when $G_p$ was bigger than 18 cm$^{-1}$. The characteristics of the gain region and that of the refraction for XRL line are displayed in Tables 1 and 2 respectively. Comparing with model Agn3, we found that $T_e$ and $\eta_{Ni}$ increased by 20% and 25%, although $T_i$ increased by 20% and $N_e$ decreased 25%, however $G_p$ increased 30%, d$x$ increased 25%. $x_p$ moved outside by ∼10 $\mu$m, d$N_e$/d$x$ and $\theta_2$ were bigger than those in model Agn3 by about 10%.

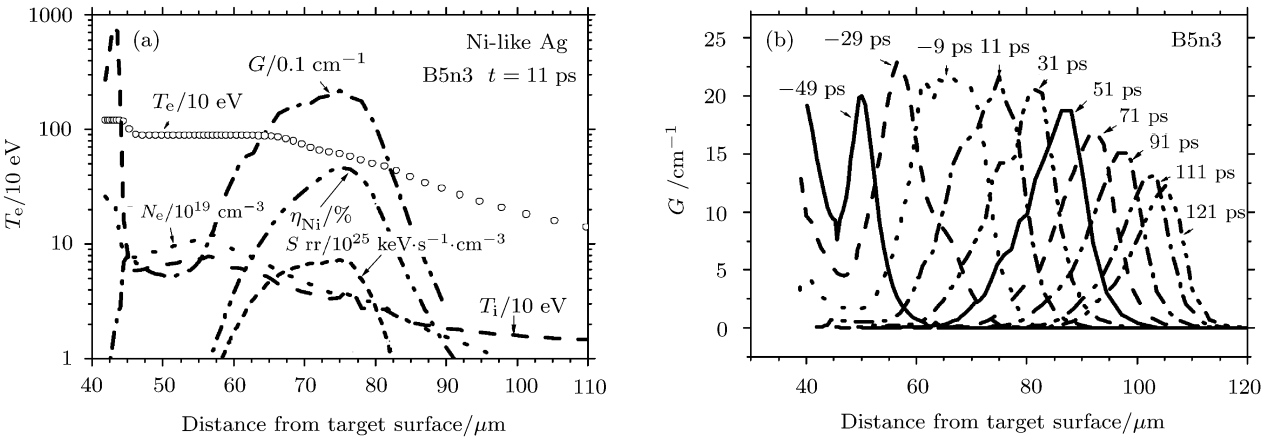



**Fig.3.** (a) Plasma status of gain region. (b) Time evolution of gain for model B5n3.

**Table 1.** The status of gain region.

| Model | $t_p$/ps | $x_p$/$\mu$m | d$x$/$\mu$m | $G_p$/cm$^{-1}$ | $T_e$/eV | $T_i$/eV | $\eta_{Ni}$/% | $N_e$/10$^{19}$cm$^{-3}$ |
|---|---|---|---|---|---|---|---|---|
| Agn3 | 6 | 66.7 | 11.3 | 16.6 | 504 | 27.8 | 37.0 | 4.17 |
| B5n3 | 11 | 75.0 | 14.2 | 21.7 | 604 | 33.9 | 46.4 | 3.66 |
| L8n3 | 17 | 82.2 | 12.4 | 22.9 | 588 | 31.2 | 46.2 | 3.81 |
| G9n3 | 21 | 74.6 | 15.7 | 20.1 | 526 | 29.8 | 46.9 | 3.59 |

**Table 2.** For 20 mm target, the estimated refraction angle and peak position in the near field.

| Model | $(\mathrm{d}N_\mathrm{e}/\mathrm{d}x)/10^{22}\mathrm{cm}^{-4}$ | $(\mathrm{d}\theta/\mathrm{d}z)/(\mathrm{mrad/cm})$ | $\theta_1$/mrad | $\theta_2$/mrad | $\theta$/mrad | $\theta_\mathrm{ph}$/mrad | $x_1/\mu$m | $x_2/\mu$m | $x_\mathrm{p}/\mu$m | $x/\mu$m | $x_\mathrm{ph}/\mu$m |
|---|---|---|---|---|---|---|---|---|---|---|---|
| Agn3 | −1.99 | 1.72 | 1.72 | 0.96 | 2.68 | 2.61 | 8.60 | 9.60 | 66.7 | 84.9 | 85.4 |
| B5n3 | −2.20 | 1.90 | 1.90 | 0.95 | 2.85 | 2.37 | 9.50 | 9.50 | 75.0 | 94.0 | 93.0 |
| L8n3 | −2.00 | 1.73 | 1.73 | 0.96 | 2.69 | 2.53 | 8.65 | 9.60 | 82.2 | 100.5 | 98.0 |
| G9n3 | −1.88 | 1.62 | 1.62 | 0.85 | 2.47 | 2.20 | 8.10 | 8.50 | 74.6 | 91.2 | 87.9 |

For the two-layer target with Al foundation, the model L8n3 with $d_\mathrm{Ag} = 4.8$ nm was best. The plasma status of gain region at $t_\mathrm{p} = 17$ ps and time evolution of gain was shown in Figs.4(a) and 4(b) respectively. It showed that near the critical surface and in the silver plasma, there both appeared a quite similar flat top each with ∼ 1550 eV and 930 eV on the curve for $T_\mathrm{e}$. Here plasma was over-ionized and $\eta_\mathrm{Ni}$ was low. The gain region was ∼70–85 $\mu$m. In the gain region $T_\mathrm{e}$ was down from 846eV to 530eV; it was ∼38% of that near the critical surface. The gain region incessantly moved outside. It lasted 110 ps, when $G_\mathrm{p}$ was bigger than 18 $\mathrm{cm}^{-1}$. The characteristics of the gain region and that of the refraction for XRL line are also displayed in Tables 1 and 2 respectively. Comparing with model Agn3, we found that $T_\mathrm{e}$ and $\eta_\mathrm{Ni}$ increased 17% and 25%, although $T_\mathrm{i}$ increased 12% and $N_\mathrm{e}$ decreased 9%, $G_\mathrm{p}$ increased 38%, $\mathrm{d}x$ increased 10%. $x_\mathrm{p}$ moved outside ∼15 $\mu$m, $\mathrm{d}N_\mathrm{e}/\mathrm{d}x$ and $\theta_2$ were almost the same as those in model Agn3.

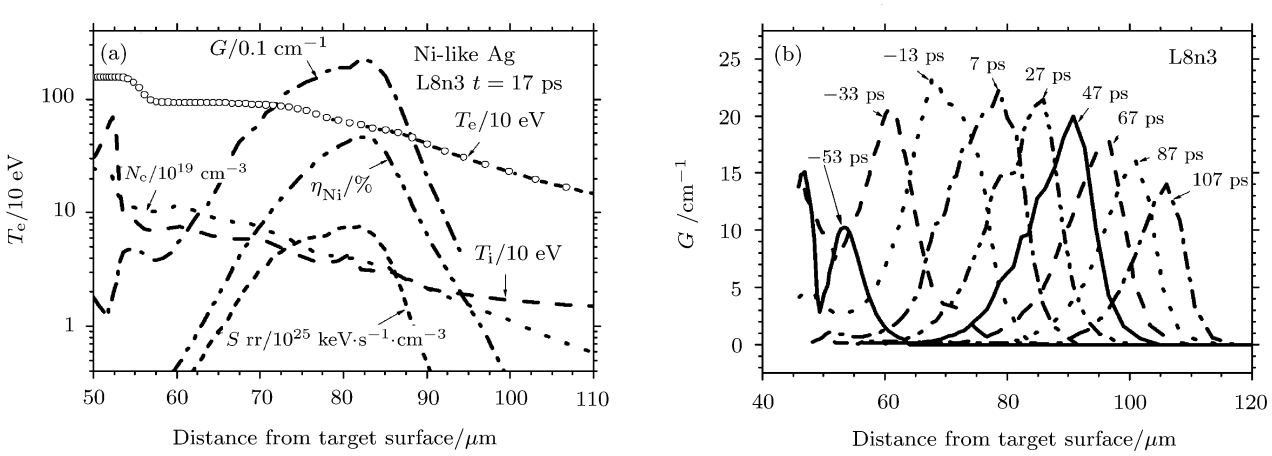



**Fig.4.** (a) Plasma status of gain region. (b) Time evolution of gain for model L8n3.

For the two-layer target with Ge foundation, the model G9n3 with $d_\mathrm{Ag}$=4.2 nm was best. The plasma status of gain region at $t_\mathrm{p}$=21 ps and time evolution of gain is shown in Figs.5(a) and 5(b) respectively. Different from the above two models, the curve for $T_\mathrm{e}$ displays one flat top near critical surface with ∼ 1810 eV, while in silver plasma, it showed a quite smooth slope. The plasma here was over-ionized and $\eta_\mathrm{Ni}$ was low. The gain region was ∼60–80 $\mu$m. In gain region $T_\mathrm{e}$ was down from 780 eV to 480 eV, approaching to ∼29% of that near the critical surface. The gain region incessantly moved outside. It lasted 100 ps, when $G_\mathrm{p}$ was bigger than 18 $\mathrm{cm}^{-1}$. The characteristics of the gain region and that of the refraction for XRL line are also given in Tables 1 and 2 respectively. Comparing with model Agn3, we found that $T_\mathrm{e}$ and $\eta_\mathrm{Ni}$ increased 4% and 27%, although $T_\mathrm{i}$ increased 7% and $N_\mathrm{e}$ decreased 14%, $G_\mathrm{p}$ increased 20%, $\mathrm{d}x$ increased 39%. $x_\mathrm{p}$ moved outside ∼8 $\mu$m, $\mathrm{d}N_\mathrm{e}/\mathrm{d}x$ and $\theta_2$ were smaller than those in model Agn3 by about 10%.

For the two-layer target with CH and Al foundation, the main reason for enhancing $G_\mathrm{ef}$ was the increase of $T_\mathrm{e}$ and $\eta_\mathrm{Ni}$, but for the two-layer target with Ge foundation, the main reason was the increase of $\eta_\mathrm{Ni}$. And one must note that for the three kinds of two-layer target, the peak intensity of spontaneous radiation intensity for the 13.9 nm laser line was larger than that for pure silver target by about 32.6%, 37.7% and 28.9% respectively.

Finally, we studied the Ne-like Ge 19.6 nm laser line. In model G9n3, $t_{\rm p}$ was $-23$ ps; at this time, the status of gain region and time evolution of gain was as shown in Figs.6(a) and 6(b) respectively. The gain region was near the critical surface and from 5 $\mu$m to 35 $\mu$m. In the gain region, $T_{\rm e}$ varied little with a difference of less than 10%. $G_{\rm p}$ was 22.0 cm$^{-1}$, $x_{\rm p}$ was 29.0 $\mu$m. At $x_{\rm p}$, $T_{\rm e}$, $T_{\rm i}$, $\eta_{\rm Ni}$ and $N_{\rm e}$ were 1319 eV, 107 eV, 61.4% and $3.74\times10^{20}$ cm$^{-3}$ respectively. d$x$ was 17.7 $\mu$m. d$N_{\rm e}$/d$x$, $d\theta$/d$z$, $\theta_1$, and $x_1$ was $-1.38\times10^{23}$ cm$^{-4}$, 23.8 mrad/cm, 23.8 mrad and 119 $\mu$m respectively. For 20 mm propagating length, most laser lines were refracted outside of the gain region. From 11 $\mu$m to 19 $\mu$m, the gain ranged from 12 cm$^{-1}$ to 14 cm$^{-1}$, $N_{\rm e}$ varied smoothly, the d$N_{\rm e}$/d$x$ was $-0.235\times10^{23}$ cm$^{-4}$, so that d$\theta$/d$z$ was 4.0 mrad/cm, for half target length, the refracted distance was 20 $\mu$m, and most laser lines were also refracted outside of the gain region. But from 12 $\mu$m to 17 $\mu$m, there was a concave distribution of electron density, which was favourable to XRL line propagation and amplification. The gain region incessantly moved outside too. It lasted 70 ps, when $G_{\rm p}$ was bigger than 16 cm$^{-1}$. $\theta_2$ was 1.4 mrad. Because of refraction, for the 19.6 nm line, although the $G_{\rm p}$ was 10% bigger than that mentioned above for the 13.9 nm line, its $G_{\rm ef}$ was 40% less than the latter one. For the two laser lines, there was a 10 mrad difference in the refracted angle, so it was easy to disjoin them. By the two-layer target with Ge foundation, two laser lines with different wavelength could be produced at one shot. By the way, for the Ne-like Ge 19.6 nm line, the best choice was 3 % prepulse and $t_{12}=7.5$ ns, and in this case, $G_{\rm ef}$ was 13.3 cm$^{-1}$.[10] In order to get the two laser lines with large intensity, further optimization is needed.

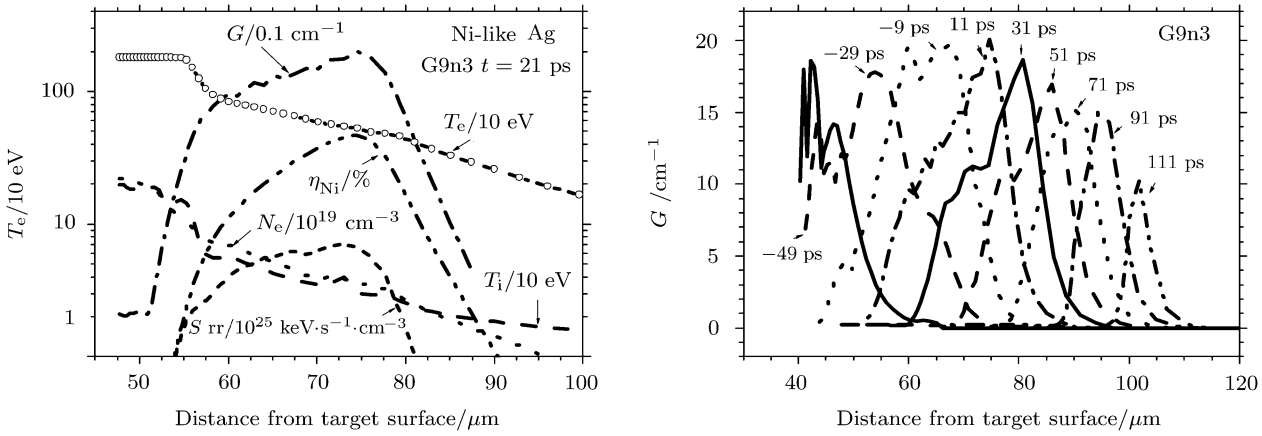



**Fig.5.** (a) Plasma status of gain region. (b) Time evolution of gain for 13.9 nm line.

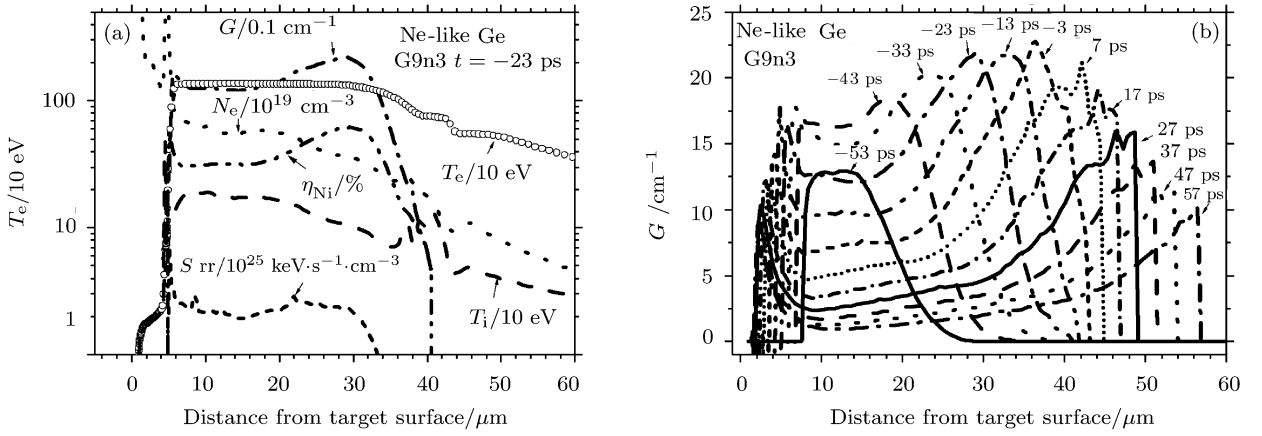



**Fig.6.** (a) Plasma status of gain region. (b) Time evolution of gain for 19.6 nm.

# 4. Conclusion

Firstly, the absorption of laser energy for two-layer target dramatically decreased, and as a result, the peak electron temperature in plasma also dramatically decreased. But on the other hand, as more laser energy was reflected near the critical surface, a larger amount of energy could be deposited in the gain region. Secondly, because such materials as CH, Al and Ge radiate less x-ray emission compared with silver, the electron thermal conduction was relatively intensified, hence the electron temperature varies very smoothly, so compared with pure silver target, the electron temperature in the gain region slightly increased, and in addition, the reduced x-ray emission resulted in increase of abundance of Ni-like ions due to less photo-ionization of the M shell electron of silver. To see the effect of photo-ionization clearly, the width of the focus line was increased, and the $G_{\rm ef}$ for pure silver target was found to decrease, but not for the two-layer target. Finally, compared with pure silver target, for 4.8 nm thickness silver, the $G_{\rm ef}$ increased by 30% for two-layer target with CH and Al foundation respectively, and for 4.2 nm thickness silver, $G_{\rm ef}$ increased by 20% for two-layer target with Ge foundation. In conclusion, the two-layer target was a good x-ray laser amplifier. For the two-layer target with Ge foundation, two saturated output laser lines at 19.6 nm and 13.9 nm could be obtained at one shot, and this may have special application in the future.

# Acknowledgments

This work was directed by Professor Yu Min. We would also like to thank Professor Li Yuemin, Yan Jun, Qiu Yubo and Fang Quanyu for providing atomic data.

# References

[1] Da Silva L B, Barbee Jr. T W, Cauble Jr R *et al* 1995 *Phys. Rev. Lett.* **74** 3991
[2] Smith R F, Dunn J, Nilsen J *et al* 2002 *Phys. Rev. Lett.* **89** 065004
[3] Wang C, Wang W, Sun J R *et al* 2005 *Acta Phys. Sin.* **54** 202 (in Chinese)
[4] Wang C, Gu Y, Fu S Z *et al* 2002 *Acta Phys. Sin.* **51** 847 (in Chinese)
[5] Zhang G P, Zhang T X and Zheng W D 2004 *High Power Laser and Particle Beams* **16** 1375 (in Chinese)
[6] Keanan R, Dunn J and Patel P K 2005 *Phys. Rev. Lett.* **94** 103901
[7] Zhang G P, Zhang T X and Zheng W D 2005 *High Power Laser and Particle Beams* **17** 1817 (in Chinese)
[8] Zhang G P, Zhang T X and Zheng W D 2006 *High Power Laser and Particle Beams* **18** 210 (in Chinese)
[9] Zhang G P, Zhang T X and Wu J Z 1998 *High Power Laser and Particle Beams* **10** 352 (in Chinese)
[10] Zhang G P, Zhang T X and Zheng W D 2004 x-ray Lasers 2004: 9th International Conference on x-ray Lasers C186 381